Excited state decay in the photosisomerization of azobenzene: a new balance between mechanisms

Josep Casellas,[a] Michael J. Bearpark,[b] Mar Reguero*[a]

[a]Departament de Química Física i Inorgànica, Universitat Rovira i Virgili. C. Marcel·lí Domingo, 1. 43007-Tarragona (Spain); E-mail: mar.reguero@urv.cat

[b]Department of Chemistry, Imperial College London, London SW7 2AZ, UK

Abstract: The mechanism of the photoisomerization of azobenzene has been studied by means of multiconfigurational ab initio calculations. Our results show that it is necessary to account for the dynamic electron correlation in the location of the critical points (CASPT2 optimizations) to obtain a correct description of the topography of the potential energy surfaces of the low-energy singlet excited states. Using this methodology, we have found that the state populated by the initial excitation is the S_2 ($\pi\pi^*$) state, which decays very efficiently to the S_1 ($n\pi^*$) state at a pedal-like non-rotated geometry. On the S_1 state, relaxation leads to a rotated geometry where the system decays to the ground state, in which further relaxation can lead to either the trans or cis geometries. However the S_1/S_0 CI seam also extends to planar geometries, so this reaction path is also accessible for rotation-constrained systems. Our results explain the experimental observations satisfactorily.

Introduction

Azobenzene is an organic compound that has a singular behaviour due to the possibility of switching between isomers using particular wavelengths of light. During this isomerization reaction, we can identify two isomers, *trans* and *cis*, with *trans* usually being the most stable one in the ground state. This isomerization process was discovered by Hartley in 1937,[1] who found that the azobenzene changed its colour when it was irradiated with sunlight, a change that could be reversed if the product was irradiated or even when kept in the dark for a certain time (Figure 1).

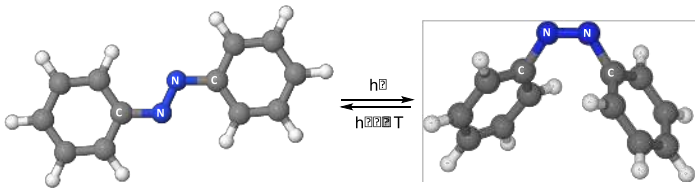

Figure 1. Azobenzene photoisomerization.

The high rate of these forward and back reactions, the fatigue resistance of the system, the stability of both trans and cis isomers and the possibility of tuning the properties of azo-derivatives by substitution, all give azo compounds a wide range of potential applications (see references 2 and 3 for recent reviews on the subject). Their applications are enlarged thanks to the readiness of these molecules to be incorporated into polymers and other kinds of materials such as liquid crystals, self-assembled monolayer or micelles, biomaterials etc., and to the possibility to tune their properties by means of ring substitution. A first series of applications are derived from the substantial change of shape of the molecule during the isomerization. The photo-mechanical properties of azobenzenes can be applied in micropumps or valves (to mimic the beat of a heart), molecular motors, wipers or articulations in robotics. Their strong electronic absorption makes them interesting candidates for light energy

harvesting and storage applications. Given that the photochromic properties can be tuned by ring substitution, azobenzene derivatives can be tailored to work in much of the solar spectrum, as solar fuels and as pigments or dyes. With appropriate ring substituents, it is also possible to modulate the back isomerization rate. If this back reaction is slow, azobenzenes can be used in information storage materials; if fast, in information-transmitting systems. If the substituents have adequate electron-donor acceptor properties, azobenzenes acquire nonlinear optical properties. This wide range of potential applications has attracted much interest in the study of their photoisomerization reactions. In spite of this and the early attempts to study this system systematically, from the experimental [4] as well as from the theoretical [5] point of view, the mechanism of this reaction is not completely clarified and works on the subject continue being published nowadays. [6,7,8]

The purpose of this article is to offer a computational perspective on the competing reaction mechanisms for the photoisomerization of azobenzene to explain the experimental observations. With this aim, the study has been performed using multiconfigurational ab initio methods. These include the effect of the dynamic electron correlation in the description of the excited states, which proves to be essential to give accurate results, and is the source of the differences found with computational works published previously.[9]

In the absorption spectrum of azobenzene itself, two major bands are found in the UV-visible region. The first is a weak band located at 430nm, corresponding to a transition to the S_1 state, of $n\pi^*$ character. The second band, at 320nm, corresponds to an absorption to the S_2 state of $\pi\pi^*$ character. This band is much stronger, given the symmetry allowed character of the $S_0 \rightarrow S_2$ transition. For systems with free rotation, a different quantum yield for isomerisation is observed for each state when they are irradiated separately: 0.20-0.27 for S_1 ($n\pi^*$) and 0.09-0.12 for S_2 ($\pi\pi^*$).[10,11] These facts suggest that two different isomerization mechanisms operate on excitation into these two electronic excited states.

Comparison of the decay factors of the reaction by direct irradiation and indirect sensitization and quantum yield measurements indicate that triplet states are not involved in the reaction mechanisms [10,12,13,14,15,16]. For a long time, it was established that the two mechanisms in play for the photoisomerization of azobenzene were in-plane inversion at one of the two nitrogen atoms when the reaction takes place by excitation to the first singlet excited state (S_1 ($n\pi^*$) state) and twisting around the N=N double bond when excited to the second one (S_2 ($\pi\pi^*$) state) (Scheme 1).

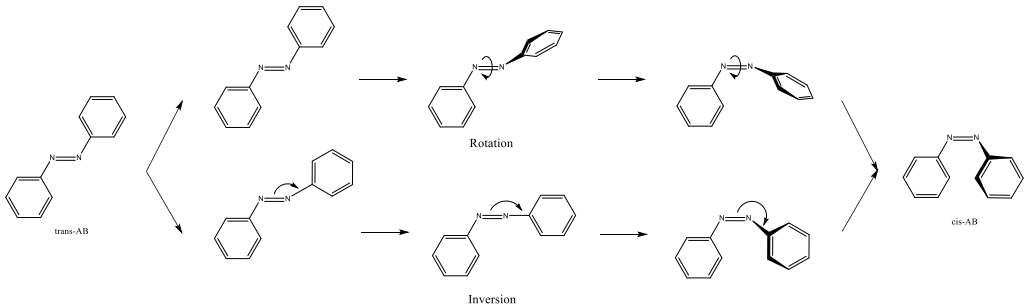

Scheme 1. Classical mechanisms proposed for the isomerization of azobenzene

This hypothesis was supported by many experimental works of that period[17,18,19,20,21,22] and by theoretical work that was very influential at that time.[23] This showed that the initial relaxation along the S_2 ($\pi\pi^*$) state corresponded to a rotation, but that soon along this downhill path, a bifurcation offers two possible deactivation channels: the first one corresponds to radiationless decay to the *trans* ground state, and the second to internal conversion to the S_1 ($n\pi^*$) state. On this surface, the rotation shows a large energy barrier, so the inversion is the only possibility to reach the *cis* product. The bifurcation along the $\pi\pi^*$ path explained, for the first time, the different quantum yields measured when the system was excited to the $n\pi^*$ or $\pi\pi^*$ excited states. This study also supported the lack of involvement of triplet states.

To further support this theory, photoisomerization quantum yields were measured for systems with restricted rotation. The results were not conclusive. On the one hand, in all cases quantum yields become almost wavelength-independent, showing the same results when exciting separately to S_1 ($n\pi^*$) or to S_2 ($\pi\pi^*$). On the other hand, using different restrictive strategies, in some cases the value obtained is the same as when excited to S_2 ($\pi\pi^*$) in free-rotation systems (0.13 approximately),[24] and in others it was equal to the value for excitation to S_1 ($n\pi^*$) in free-rotation systems (between 0.21-0.24).[11,25] As a result, whether rotation is completely or only partially precluded is not clear.[26]

Later works suggested that other processes were also possible. The computational location of an S_1 ($n\pi^*$)/S_0 conical intersection at a geometry with a 90º value of the dihedral CNNC angle suggested that rotation could dominate the reaction coordinate along the $n\pi^*$ surface.[27] The location, also computationally, of a crossing between the S_2 ($\pi\pi^*$) state and a doubly-excited $n^2\pi^{*2}$ state, suggests the involvement of this latter state in the photoisomerization, which could explain the different lifetimes and the lower quantum yield of isomerization when azobenzene is excited to the $\pi\pi^*$ state, in competition with the efficient conversion from the $n\pi^*$ state to the *cis* ground state.[27,28] In addition, some experimental works, based on femtosecond fluorescence anisotropy measurements, support the hypothesis of a rotation mechanism on S_1 ($n\pi^*$),[29] or even decay from this state in a bi-phasic fashion,[30] contradicting previous experimental results.[21,22]

Trying to clarify arguments in the debate, Schultz[31] stated in a simple way the facts that proposed mechanisms for azobenzene photoisomerization should explain: first, the wavelength dependence of the quantum yields; second, the changes when the rotation is blocked (although there were doubts about the real blockage of rotation of the constrained azobenzene derivatives used in some studies[23]). Finally, it should be born in mind that the quantum yield of internal conversion from $\pi\pi^*$ to $n\pi^*$ is equal to one and that the crossing point between these states has to be planar, and that the involvement of higher energy states could be crucial for the mechanism.

Since then, more theoretical work has been carried out to investigate the photochemistry of azobenzene, from the stationary point of view, studying the potential energy surfaces of the low-energy states[32,33,34,9] or running dynamics calculations.[35,36,37,38,39,40,41] Based on these works, other mechanisms, different from pure rotation or inversion, have been proposed (Scheme 2), such as inversion assisted rotation,[32] concerted inversion where both NNC angles invert at the same time,[33] or rotation helped by the opening of the CNN angles.[35] In fact, mixed mechanisms are in general suggested by the results of dynamic studies.[36,37,38,39,40,41] Alternative paths for the same mechanisms are also suggested, based on new conical intersections or stable intermediates found: a $S_2(\pi\pi^*)/S_3(n^2\pi^{*2})$ CI near the FC geometry indicates that perhaps there is no path for isomerization on the $S_2(\pi\pi^*)$ surface,[34] while a series of planar conical intersections $n^2\pi^{*2}/n\pi^*$ and $n\pi^*/S_0$ are the key features to propose a mechanism without the assistance of a $n\pi^*/\pi\pi^*$ intersection, the existence of which was precluded,[9] in opposition to other works where a planar $n\pi^*/\pi\pi^*$ crossing point is reported.[39] A new excited species described by means of a pedal-like deformation that could be involved in the isomerization reaction was also found.[6,40,41]

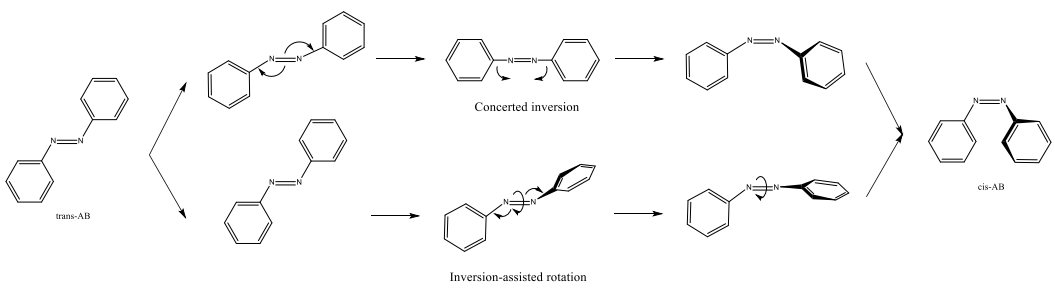

Scheme 2. Novel mechanisms proposed for the photoisomerization of azobenzene

The most recent computational[7,42] and experimental[8] works are focused on the dynamics along the nπ* state. In general, all of them agree in suggesting that the rotation is the main coordinate of decay from S_1 to S_0 followed by subsequent isomerization, although some authors indicate a certain involvement of secondary coordinates like displacement of the N-N moiety[42] or inversion.[8] The evolution of the system when excited to the ππ* state is less studied, but the few works that focus on it also states the importance of secondary coordinates like rotation of phenyl groups.[6] In this landscape, the detailed mechanism of the photoisomerization of azobenzene remains an open question.

This article revisits the study of the mechanism of photoisomerization of azobenzene on its S_1 (nπ*) and S_2 (ππ*) excited states from the computational point of view. We have determined the topography of the potential energy surfaces (PES) of these low-energy states of the system by means of an ab initio methodology that includes dynamic electron correlation. This effect has been shown to be crucial in the correct determination of relative energies when states of different nature are involved in the phenomena studied,[43,44] as is the case here, where nπ* and ππ* states interplay. Not including dynamic correlation can change the topography of the PES, changing the location of the minima and the shape of the reaction paths. Our results show that this is the case for azobenzene, where the main relaxation coordinate along the S_1 (nπ*) state changes when dynamic correlation is considered in the energy calculation, which is likely to be the origin of contradictory computational results in previous theoretical works.

Specifically, we have used in general the CASSCF/CASPT2 (Complete Active Space Self Consistent Field/CAS second-order multiconfigurational perturbation) combined methodology, optimizing - for the first time to our knowledge - some of the critical points of the excited states at the MS-CASPT2 level. This strategy allows accurate and balanced energies for the different states involved in the reactivity and for the different areas of the PES that must be analysed in the study of this photochemical reaction to be obtained. Our results explain most of the experimental observations and are consistent with the experimental data available.

Computational Strategy

We have performed the study of the photoisomerization of azobenzene using the CASSCF/CASPT2 protocol. The standard application of this methodology uses the CASSCF method to optimize the critical points of the different potential energy surfaces of the states involved in the reactivity, then the energies are recalculated at these geometries at the CASPT2 level to take into account the effect of the dynamic electron correlation. This procedure has proved to be very accurate when CASSCF describes properly the electronic configurations of the states and the effect of the dynamic correlation (included as a perturbation in the CASPT2 method) is small. On the other hand, if the CASPT2 correction of the energy is large, it indicates that CASSCF does not describe the electronic state accurately and the geometries optimized at this level are not so reliable. This is the case for some of the low-lying electronic excited states of azobenzene, specifically, the S_1 (nπ*) and S_2 (ππ*) states. For these, the geometry optimizations were performed at the CASPT2 level. These optimizations provide a topography of the S_1 and S_2 surfaces quite different from the ones determined at the CASSCF level, given the different location of the minimum energy structures optimized.

To include the whole π system of azobenzene in the orbital active space, we would need to take into account 18 electrons in 16 orbitals. Unfortunately, to use this size of active space in standard calculations is unaffordable at present, so the active space was cut back; extracting those orbitals with occupations that did not change noticeably from 2 of from zero in the regions of the PESs explored of the states considered. The result was an active space of 10 electron in 8 orbitals, composed of two π and two π* orbitals of the benzenes, the π and π* of the azo group and the orbitals of the lone pairs of the nitrogen atoms. This is slightly smaller than the largest active spaces used in previous works (14 electrons in 12 orbitals used in ref. 9), but larger than others (CAS(6,6) used in refs 28 and 33. Test calculations performed for a similar system studied simultaneously by the group, phenylazopyridine, showed that bigger active spaces do not give noteworthy differences in energies or geometries.

We use the multistate version of the perturbative method (MS-CASPT2) to allow for the interaction of CASSCF states.[45] In all cases, a Pople split basis set 6-31G(d) has been used. The CASPT2 reference wave functions and the molecular orbitals were obtained by state averaged CASSCF calculations. In order to explore all the possibilities of the mechanism, symmetry constraints were not used explicitly, although trans-azobenzene presented C_{2h} geometry. The PESs between critical points of interest were explored using linear interpolation of internal coordinates (LIIC). Minimum energy paths (MEP) were also computed in some cases. In all the MS-CASPT2 calculations an imaginary shift of 0.1 was added to the zero order Hamiltonian in order to preclude the inclusion of intruder states.[46] The RAS state interaction (RASSI) protocol was used to compute the transition oscillator strengths in order to compare transition probabilities among the states studied.[47] Frequency calculations were also run to determine the nature of the stationary points. These calculations and the MS-CASPT2 optimizations were done with numerical gradients due to the lack of implementation of analytical gradients with this protocol. To make these calculations affordable computationally, Cholesky decomposition of the two-electron integral matrix has been used. All CASPT2 calculations were performed using the MOLCAS 7.6 package. [48]

Conical intersections and transition states were optimized using the algorithm[49] implemented in Gaussian 09.[50] For the first, state averaged orbitals were used and the orbital rotation derivative contribution to the gradient (which is usually small) was not computed. Full diagonalization was suppressed in order to be able to run these calculations with an affordable cost. Using the methodology described above, the four lowest-energy states were studied: S_0 (ground state), S_1 ($n\pi^*$), S_2 ($\pi\pi^*$) and S_3 ($n^2\pi^{*2}$). The latter state was also considered because, although at the Frank Condon geometry its energy is high, it crosses with the lower states along the reactive path, so it may play a role in the photoisomerization mechanism of interest.

CASSCF vs. CASPT2 results in critical cases

As mentioned above, the poor description by CASSCF of some states can make the CASSCF/CASPT2 strategy not reliable to properly describe the topology of certain PESs. In the present study this was the case for states S_1 ($n\pi^*$) and S_2 ($\pi\pi^*$). This problem is illustrated by the results presented in this section. Table 1 shows the vertical energies of the four lowest-energy states computed at CASSCF and MS-CASPT2 levels at the ground state minimum of *trans*-azobenzene. The large difference between the excitation energy calculated for the S_2 ($\pi\pi^*$) state at the CASSCF and CASPT2 levels indicates that dynamic electron correlation is very important in this state, so already the CASSCF method with the active space chosen will not provide an accurate enough description. In fact, when this state is optimized at the CASSCF level, the minimum energy point shows a structure with a clear lengthening of the N=N distance, noticeably shortened C-N_{azo} distances and with co-planar phenyl rings (Figure 2b), whereas single point energy calculations at the MS-CASPT2 level showed that the energy was lower at non-coplanar geometries, demonstrating the inadequacy of the CASSCF method to describe the S_2 PES. S_2 ($\pi\pi^*$) geometries were not optimized in previous computational works, where only scans were performed, so these results cannot be compared with similar ones.

Table 1. Energies of the three lowest excited states relative to the ground state (in kcal·mol^{-1}) calculated at CASSSCF and CASPT2 levels at the S_0 *trans*-minimum.

State	Character	CASSCF	MS-CASPT2
GS		0.0	0.0
S_1	$n\pi^*$	71.5	65.9
S_2	$\pi\pi^*$	142.0	96.3
S_3	$n^2\pi^{*2}$	157.6	151.3

Although the dynamic correlation does not affect so strongly the S_1 ($n\pi^*$) energies at the Franck-Condon geometry (FC), the CASSCF geometry optimization for this state showed the same problems as for the S_2 ($\pi\pi^*$) state. The minimum energy geometry found at the CASSCF level shows a planar structure (Figure 2a), approximately 52.5 kcal·mol^{-1} above the ground state minimum and 13.1 kcal·mol^{-1} more stable than its energy at FC. In this structure the C-N_{azo} bonds are shortened, but there is almost no change in the N=N one, which keeps the double bond character, precluding rotation around it. The NNC angle is slightly larger than in S_0. This geometry is the one reported as the S_1 ($n\pi^*$) minimum in previous works[9,28,33] where the topography of the PESs was explored exclusively using the CASSCF method. This structure suggests that inversion could be the preferred mechanism along this surface, which would be in agreement with the initial hypothesis about the photoisomerization mechanisms in azobenzene. But when energies are recalculated at the MS-CASPT2 level, the profiles of this PES show that rotation decreases the energy of S_1 at the same time as the N-N distances increases up to 1.30 Å, which indicates that CASSCF does not describe the topography properly and that rotation is possible along this surface. Consequently, CASPT2 optimizations are necessary also for S_1. In fact, the minimum found at the latter level is more than 5 kcal·mol^{-1} more stable than the structure optimized at CASSCF level.

On the other hand, the minimum of the S_3 state, unlike the other cases, presents a geometry with the CNNC dihedral angle near 90 ° at the CASSCF level. The correct location of this minimum in this region of the PES was corroborated by the MS-CASPT2 calculated profiles of this surface. Consequently, this minimum was not reoptimized at the CASPT2 level.

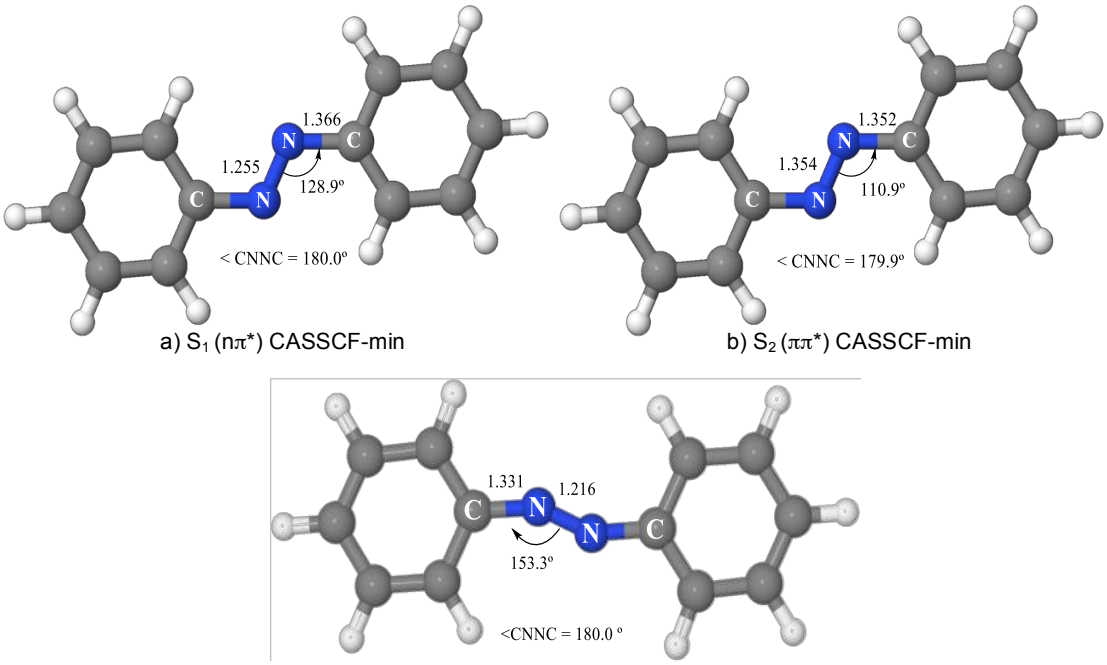

a) S_1 ($n\pi^*$) CASSCF-min

b) S_2 ($\pi\pi^*$) CASSCF-min

c) S_1 ($n\pi^*$)/S_0 planar CASSCF CI

Figure 2. Geometries of critical points optimized at CASSCF level.

A direct consequence of the poor description of some states at the CASSCF level is that at the CASSCF-optimised conical intersections, the CASPT2 states are far from degenerate. The most unfavourable case found in this work corresponds to a S_1 ($n\pi^*$)/S_0 CI with a planar structure located at the CASSCF level (Figure 2c), that showed a gap between states of 10 kcal·mol^{-1} when the energies were recalculated at CASPT2 level. In this and similar cases, the location of near crossing points has been accomplished exploring the neighbouring region of the PES with grid calculations at the CASPT2 level. It means that the energy of these points give us an upper limit for the minimum energy of the crossing, given that they are not fully optimized with CASPT2.

Results and Discusion

In this work we want to elucidate the mechanisms of photoisomerization of azobenzene in different conditions. First we have to take into account the possibility of the system being excited to the first or to the second excited state. Then we have to consider also the cases of free-rotating and rotation-constrained systems. The results will be organized according to these possibilities. We will first localize the minima on the ground and excited state surfaces, which correspond to stable species. We will also locate the points where the different surfaces cross, that open the channels for radiationless deactivation processes. Then we will explore the connections between the different critical points located (obtaining the profiles of the surfaces along the LIICs that join those points) to see if the system could evolve along those paths. We will first explore the relaxation processes along the S_1 and S_2 PES from the Frank Condon geometry. Then we will explore the paths from the minima populated by these relaxations to the points of radiationless deactivation (crossing points). They must lead, eventually, to the ground state surface, where the system will evolve towards the initial reactant (*trans* isomer) or to the photoproduct (*cis* isomer). The back-isomerization along the ground state surface is also analysed. This is one of the first processes studied, because the information obtained from it will be useful to understand some of the processes studied afterwards.

These paths will be obtained first without imposing any geometrical restriction. To elucidate the photoisomerization mechanism for rotation-constrained systems, we will have to find, following a similar scheme, alternative paths where the CNNC dihedral angle is kept to 180º.

The reaction paths found for all these cases must explain the experimental facts observed.

All the energies given in this section correspond to MS-CASPT2 results, unless explicitly indicated otherwise.

Ground state minima

The geometry optimization of the ground state of the trans and cis isomers gave the structures depicted in Figure 3. The *trans* isomer is 14.3 kcal·mol^{-1} more stable than the *cis* one. *Trans*-azobenzene shows a planar structure, while in the *cis* isomer both benzene rings show a conrotatory twist around the C-N=N-C moiety. In fact, the central link is not completely planar, given that the dihedral angle C-N=N-C is 3.2 degrees.

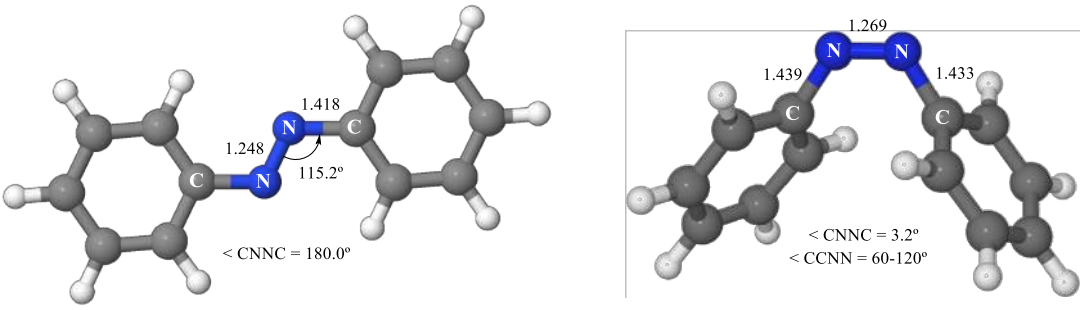

a) S_0 *trans*-min b) S_0 *cis*-min

Figure 3. a) Ground state trans global minimum b) cis minimum. Both optimized at CASSCF level.

The main parameters of the geometry obtained for the *trans* isomer can be compared with data obtained from gas-phase electron diffraction.[51] The experimental values of N-N and C-N bond distances (1.260 Å and 1.427 Å respectively), NNC angle (114º) and CNNC dihedral angle (180º), are in good agreement with our computational results.

At the FC geometry of the *trans* isomer, the calculation of the vertical excitations gave the results collected in Table 2. The analysis of the wave functions indicates that the excitations that give rise to the lowest energy

excited states have ($n\pi^*$), ($\pi\pi^*$) and ($n^2\pi^{*2}$) character respectively. Figure 4 shows the molecular orbitals involved in them. The oscillator strengths calculated show that the state that will be populated after the initial excitation is mainly the S_2 ($\pi\pi^*$) state. These results are in a satisfactory agreement with the experimental absorption spectra. The vertical energies obtained computationally can be compared with the absorption energies of *trans*-azobenzene reported from spectroscopic measurements. Values between 52.8 kcal·mol^{-1} and 63.5 kcal·mol^{-1} are reported for the $n\pi^*$ band, while for the $\pi\pi^*$ band the absorption energies oscillate between 86.1 kcal·mol^{-1} and 92.9 kcal·mol^{-1}.[8,10,16,19,21] Although the computed values (65.9 kcal·mol^{-1} and 96.3 kcal·mol^{-1} respectively) are in both cases larger than the experimental ones, this margin of error is not unexpected for two reasons: first, the maximum of a band does not correspond exactly with the computed vertical energy and second, in flexible systems the reproduction of the spectrum cannot be achieved by a single geometry calculation, given that in a real sample there will be a large range of geometrical deformations. This is also the reason why the observed intensity of the $n\pi^*$ band of *trans*-azobenzene is larger than predicted, given that flexibility allows the molecule to break planarity, weakening the selection rules imposed by symmetry and making the $S_0 \rightarrow n\pi^*$ transition allowed, while in the calculation of the vertical energies only a planar geometry is considered, yielding a strongly forbidden $S_0 \rightarrow n\pi^*$ transition.

Table 2. Relative energies (in kcal·mol^{-1}) of the lowest states of azobenzene at the critical points located on S_0 and oscillator strengths (f) for the transitions to the three lowest excited states at the S_0 *trans* and *cis* isomers.

		***trans*-azobenzene**		***cis*-azobenzene**		**TS**	**planar-TS**
State	**Character**	**ΔE**	**f**	**ΔE**	**f**	**ΔE**	**ΔE**
GS	-	0.0	-	14.3	-	45.3	55.0
S_1	$n\pi^*$	65.9	$0.1\cdot10^{-4}$	81.6	$0.6\cdot10^{-1}$	71.3	72.0
S_2	$\pi\pi^*$	96.3	1.27	124.1	0.21	160.2	144.5
S_3	$n^2\pi^{*2}$	151.3	$0.1\cdot10^{-4}$	157.3	$0.2\cdot10^{-1}$	127.0	123.3

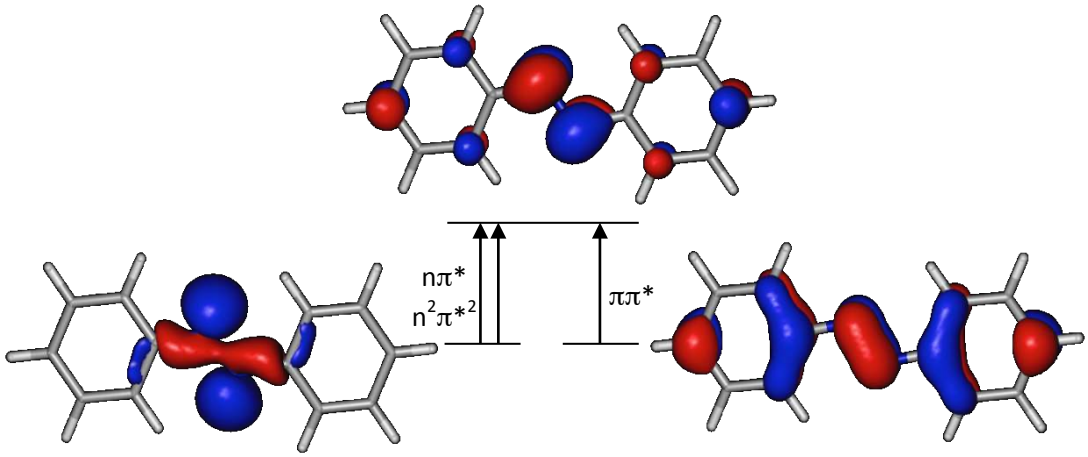

Figure 4. Molecular orbitals of the active space that are involved in the excitations that describe the electronic character of lowest energy excited states.

Critical points on excited state surfaces

Geometry optimizations without constrains were carried out for the excited states, starting at the trans FC geometry.

For the S_1 ($n\pi^*$) state, a rotated minimum with a CNNC dihedral angle of 90.1º and an elongated N-N bond was located (Figure 5a), stabilized by more than 15 kcal·mol^{-1} relative to the Frank-Condon energy of this state (Table 3). The relaxation path from FC to this minimum is barrierless. These results are in disagreement with the traditional view established by Monti et al in their computational work[23] that ruled out rotation for this state due to the presence of large energy barriers. In more recent works developed with more accurate methodologies, the S_1

PES along the rotation coordinate shows a flat profile,[32,33] but in any of these last studies the S_1 minimum was located at rotated geometries (probably due, as previously commented, to the use of the CASSCF method to optimize geometries) (see Table 2). Our geometry can be compared with that "reconstructed" in ref. 8 from experimental data, keeping in mind that results on that work does not contemplate asymmetry in the reported geometrical parameters. For both, the experimental and computational results, C-N bond distances decrease upon excitation (from 1.428 Å to 1.365 Å for the first, and from 1.418 Å to 1.399 Å /1.367 Å for the second), while N-N distance hardly changes in the experimental results (from 1.260 Å to 1.262 Å) while computationally a clear increase is predicted (from 1.248 Å to 1.301 Å). NNC angle increases also in both cases, from 114º to 124º experimentally, and from 115º to 116º/132º computationally. Unfortunately, the most crucial geometrical parameter, the CNNC dihedral angle, is not reported in that reference.

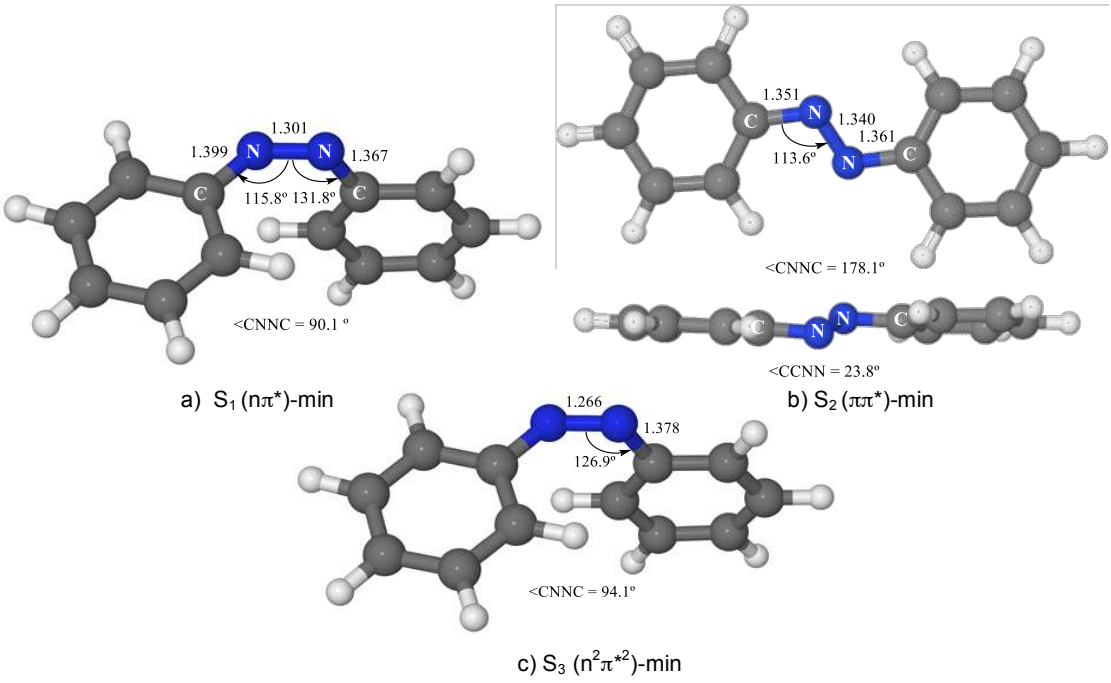

Figure 5. Minimum energy geometries of the lowest excited states of azobenzene. Optimizations run at MS-CASPT2 level for S_1 and S_2 and at CASSCF level for S_3.

At the S_1 ($n\pi^*$) minimum, the S_1 and S_0 states are almost degenerate (Table 3). A point of degeneracy between these states was optimized at the CASSCF level, located very near this minimum. This crossing point was confirmed with MS-CASPT2, lying only 1 kcal·mol^{-1} above the S_1 ($n\pi^*$) minimum. Based on a CASSCF optimization for the S_1/S_0 CI constrained to planar geometries, a planar point of degeneracy was also located (at CASPT2 level), 20 kcal·mol^{-1} above the $S_1(n\pi^*)$ minimum. Their geometries are represented in Figure 6 and the energies collected in Table 3.

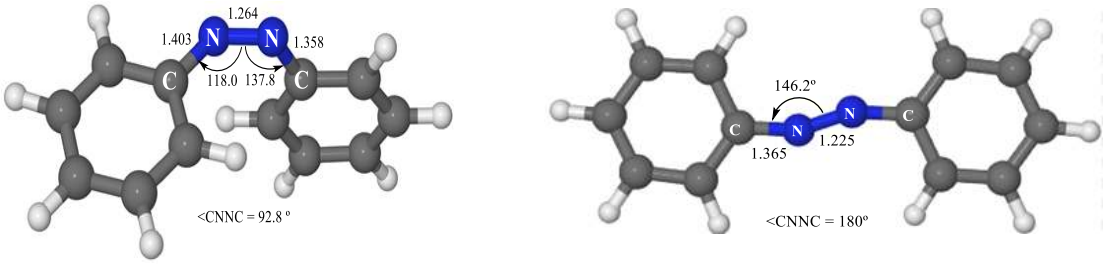

Figure 6. Points of the S_1 ($n\pi^*$)/S_0 conical intersection: a) Rotated geometry (optimized at CASSCF level); b) Planar geometry (located at CASPT2 level).

Table 3. MS-CASPT2 relative energies (in kcal·mol^{-1}) of the critical points located on the ground state and lowest energy excited states of azobenzene.

	Geometries			
	S_0 - min	S_1 ($n\pi^*$) - min	S_2 ($\pi\pi^*$) - min	S_3 ($n^2\pi^{*2}$) - min
GS	**0.0**	46.8	3.9	47.1
$n\pi^*$	65.9	**49.4**	66.7	53.7
$\pi\pi^*$	96.3	161.6	**70.3**	151.6
$n^2\pi^{*2}$	151.3	69.3	122.4	**61.7**

	Geometries			
	S_1 ($n\pi^*$)/S_0 Rotated CI	S_1 ($n\pi^*$)/S_0 Planar CI	S_1 ($n\pi^*$)/S_0 Linear CI	S_2 ($\pi\pi^*$)/S_3 ($n^2\pi^{*2}$) CI
GS	**50.5**	**69.4**	**93.0**	13.3
$n\pi^*$	**51.5**	**70.4**	**93.9**	54.1
$\pi\pi^*$	144.5	123.9	128.6	**85.8**
$n^2\pi^{*2}$	75.5	102.7	144.9	**88.6**

In the case of S_2, we find that the relaxation of the bright state does not lead to a rotation, but instead to an out-of-plane concerted distortion of CCNN and NNC'C' dihedral angles, keeping both benzene rings in parallel planes, in a pedal-like motion (Figure 5b). This movement does not match any of the prevalent mechanisms previously proposed for the isomerisation of azobenzene. Although this coordinate has been mentioned in previous works,[6,40,41] its description there is different from the one provided by our results.

We can compare some geometrical parameters of this structure with those "reconstructed" in ref. 8 for the S_2 minimum. In this case the trend of change on C-N and N-N bond distances in the same in both cases: decrease for N-C distance (from 1.428 Å to 1.373 Å in the reconstructed geometry, and from 1.418 Å to 1.361/1.351 Å in the computational one) and increase for the N-N bond length (from 1.260 Å to 1.324 Å in the reconstructed geometry, and from 1.248 Å to 1.340 Å in the computational one). NNC angle hardly changes in any case (from 114º to 112º in the reconstructed geometry, and from 115º to 114º in the computational one).

In the area around the pedal-like structure, S_1 and S_2 are almost degenerate, so it could be the case that this geometry does not, in fact, correspond to a minimum for the $\pi\pi^*$ state, but rather a minimum on the S_2 surface due to a nearby S_2/S_1 conical intersection. It is difficult to determine the exact point of crossing given that the n and π atomic orbitals of the N atoms are mixed in this distorted geometry. Nevertheless, a search in this zone did not locate any minimum of $\pi\pi^*$ character on S_1.

The minimum of the ($n^2\pi^{*2}$) state (S_3 at FC geometry) presents a geometry with CNNC dihedral angle near 90º (see Figure 5c) similar to that of the S_1 minimum. At this geometry, this state is the second excited state, which means that a crossing with the $\pi\pi^*$ state must have happened. This CI could not be optimized due to the poor description of the $\pi\pi^*$ state at CASSCF level. We located a low-energy geometry of this intersection at a rotated CNNC dihedral angle of 140º (

Figure 7). This crossing point shows elongated N-N distance, asymmetrical shortened C-N distances and opened NNC angles. The energy of this point is 9 kcal·mol^{-1} lower than the excitation energy to the S_2 state at FC geometry (15 kcal·mol^{-1} above the pedal-like S_2 minimum).

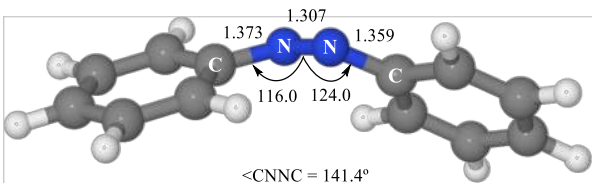

Figure 7. S_2 ($\pi\pi^*$)/S_3 ($n^2\pi^{*2}$) crossing point geometry located (not optimized) at MS-CASPT2 level.

To study the isomerisation mechanism, the paths connecting the *trans* and *cis* isomers were searched for on the ground and excited states PES.

Mechanism of Isomerization along the ground state

On the ground state surface, the transition state between cis and trans isomers was located at a geometry where the NNC angle of one of the phenyl groups is 180º. This ring is perpendicular to the rest of the molecule (azo + phenyl), as shown in

Figure 8a. The barrier of the *cis*-to-*trans* isomerization is, according to our results, is of 31.0 kcal·mol^{-1}, in reasonable agreement with the 23-24 kcal·mol^{-1} deduced from experimental measurements.[10,11] The rotation of the phenyl is a relatively inexpensive process, requiring only 5 kcal·mol^{-1} at the *cis* isomer. When this planarization is imposed on the TS, the energy of the stationary point optimized (shown in

Figure 8b) is 10 kcal·mol^{-1} higher than the previous one due to the steric repulsion of the rings. These energies are shown in Table 2. Based on these results, we conclude that the inversion mechanism is an appropriate way to carry out the thermal back-isomerization.

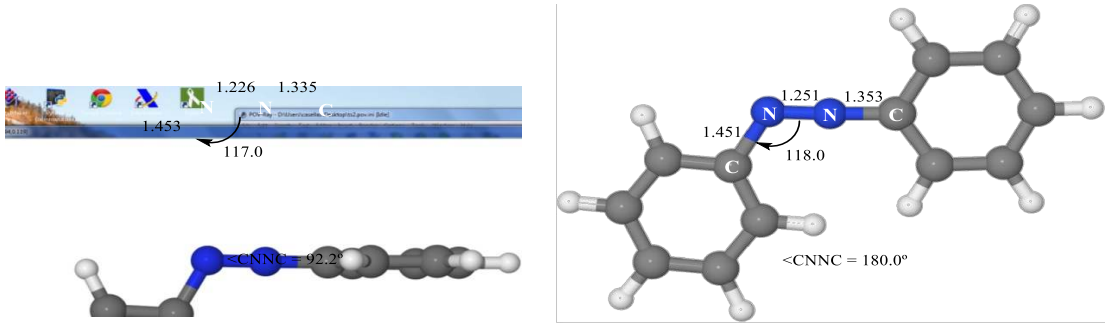

a) TS_{S0} b) planar-TS_{S0}

Figure 8. a) TS on S_0 along the inversion coordinate, b) TS on S_0 constrained at planar geometry.

Mechanism of photoisomerization for systems with free rotation

Mechanism along S_1 ($n\pi^*$) state

When the system is excited to the S_1 state (weak transition, but it can still be done[4,11,21,52]), the relaxation on this surface leads to a 90º rotated minimum, where the crossing with the ground state is nearby. The profiles of the PESs of the lowest energy states connecting the *cis* and *trans* isomers through the rotational pathway were calculated (Figure 9). The interpolation between these two geometries was carried out changing the rotation angle and optimizing the geometry of the ground state at the DFT level, keeping frozen the value of the rotation angle (these profiles of the excited states must not then be interpreted as reaction paths for these states). MS-CASPT2 energies were calculated at each and every optimized point.

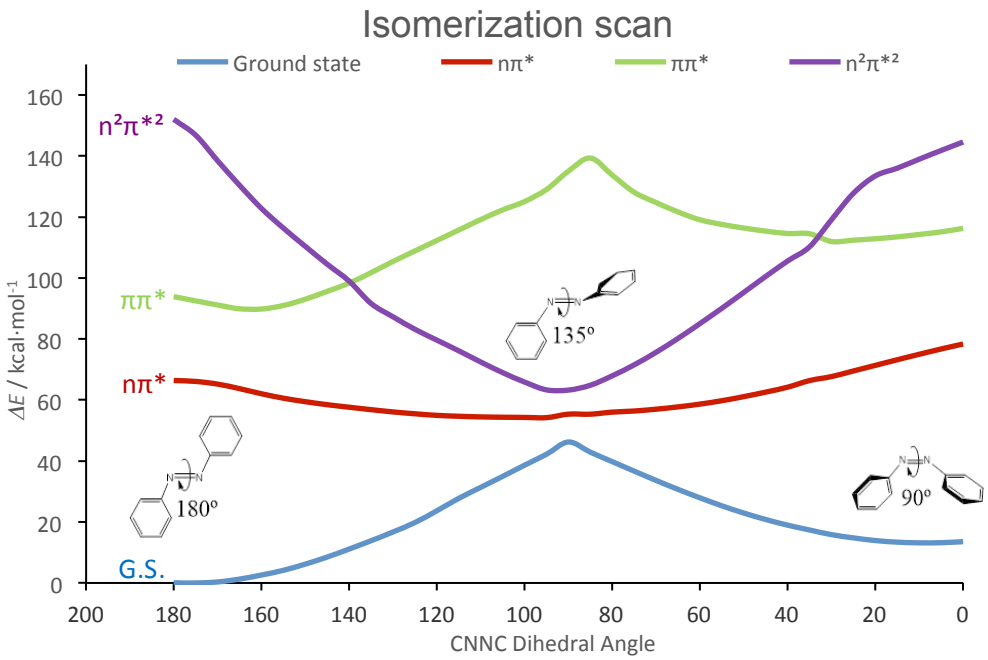

Figure 9. Profiles of the PES of the lowest energy states along the path of the rotation mechanism of the trans → cis isomerisation of azobenzene. The geometries were obtained optimizing at DFT level the geometry of the ground state for a fixed value of the rotation angle. At each geometry, the energies of the different states were calculated at the MS-CASPT2 level.

The lowest energy point of the profile of the S_1 state is located at an angle of 90º, the same rotation as that of its absolute minimum. In order to double-check this result, we traced a LIIC between the FC geometry and S_1 MS-CASPT2 minimum (Figure 10). It has to be pointed out that in the profiles shown in Figure 9, relaxation is allowed for the ground state, so it is expected the twisted near-degeneracy to be higher in energy than if optimising on S_1, as shown in Figure 10.

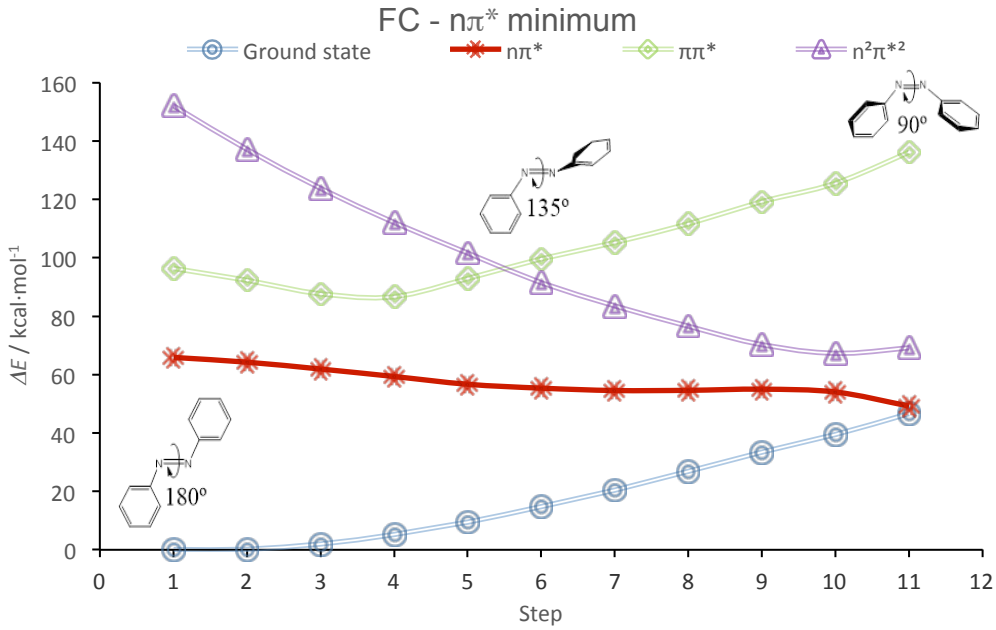

Figure 10. Profiles of the PES of the lowest energy states along a linearly interpolated path from the Franck-Condon geometry to the S_1 (nπ*) state rotated minimum.

In conclusion, when the system is excited to the (nπ*) state, it will follow the C-N-N-C rotation coordinate to the surface minimum if rotation is not hindered. Close to this minimum there is a conical intersection (geometry in Figure 6a) with S_0 where the population is funnelled to the ground state surface. This CI is located only 1-2 kcal·mol^{-1} above the nπ* minimum. The observations of the most recent experimental work on azobenzene agree remarkably well with the presence of a barrier of this small magnitude.[8] Due to the inertia of the movement, part of the system can continue to the *cis* minimum, although the *trans* isomer is favoured thermodynamically. In addition, when the *cis* form is obtained, it can revert to *trans* with the excess kinetic energy likely to be available. This would explain the low quantum yield of the photoisomerization. Anyway, it is not clear what branching of population will take place at the crossing. For this reason it would be very interesting to run dynamics based on this description of the PES, but unfortunately this calculation is not yet feasible, given the size of active space required. The mechanism described up to here is only possible for systems where rotation can take place.

Mechanism along S_2 (ππ*) state

When azobenzene is excited to the ππ* state, the minimum energy path leads to the pedal-like minimum. The relaxation from the FC geometry along the S_2 surface to this minimum does not show any energy barrier, as can be seen in the LIIC represented in

Figure **11** (S_2 – green bold line). The tendency of the system to populate this minimum after the initial excitation has been confirmed by a Minimum Energy Path calculation run on the S_2 surface from the FC structure.

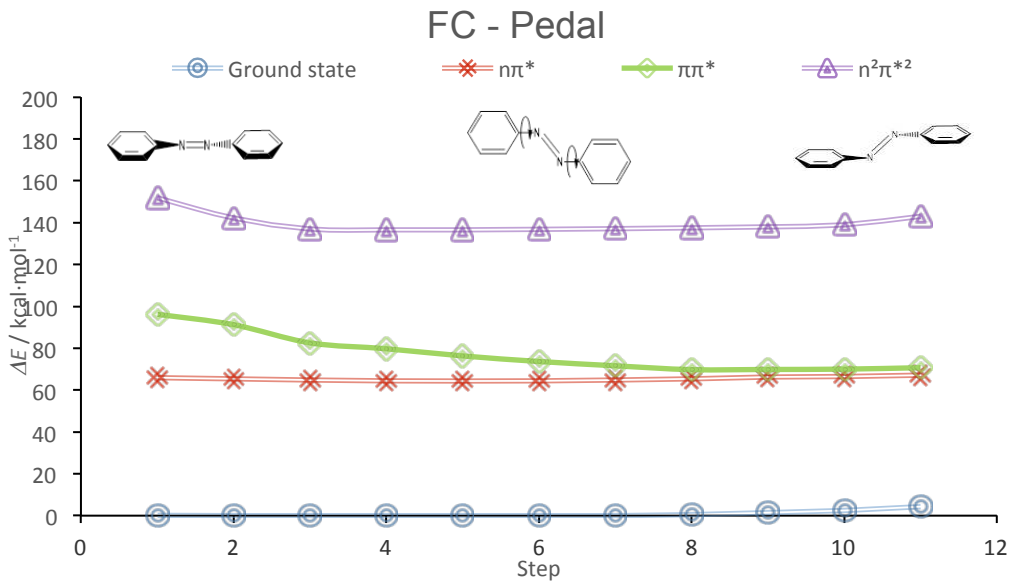

Figure 11. Profiles of the PES of the lowest energy states along the path from the Franck-Condon geometry to the pedal-like structure.

Given that in the surroundings of this geometry S_1 and S_2 are degenerate, the crossing to the S_1 (nπ*) state will be fast and efficient. To check if from this geometry the S_1/S_0 CIs are accessible, we calculated the profile of the S_1 surface along the LIIC between the S_2/S_1 CI and rotated S_1/S_0 CI. As shown in Figure 12, the path is barrierless, so this decay path is probable. From this point, the evolution of the system is the same than when excited to S_1 (nπ*).

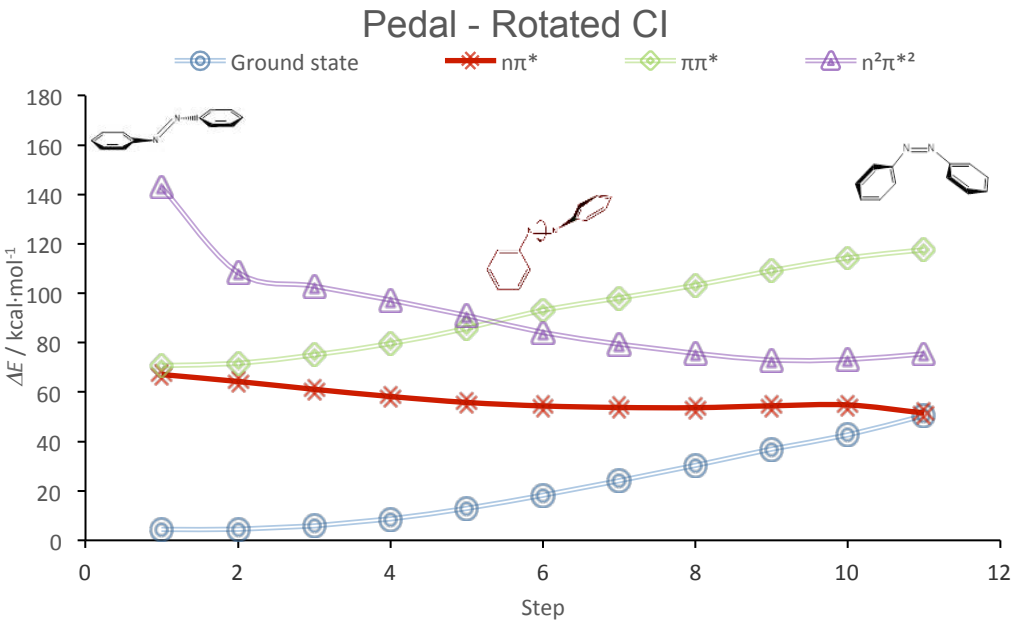

Figure 12. Profiles of the PES of the lowest energy states along the path from the pedal-like structure to the S_1/S_0 rotated CI.

Although at the FC geometry the gradient of the S_2 surface leads towards the planar pedal-like minimum, there is another down-hill direction that corresponds to small rotation. In fact, the energy of the S_2 ($\pi\pi^*$) state decreases with rotation until 160º, where a local minimum is placed. If this path is followed, the system can cross to the $n^2\pi^{*2}$ surface, given that the S_3/S_2 CI is located near the $\pi\pi^*$ state local minimum, only 5 kcal·mol^{-1} above it, and 9 kcal·mol^{-1} less energetic than the initial excitation as shown in Figure 13. From this point, the population can reach the $n^2\pi^{*2}$ surface minima that shows a C-N-N-C dihedral angle of 90°. At this minimum, the S_3 state is only 10 kcal·mol^{-1} higher in energy than S_1 ($n\pi^*$). This small gap seems to be maintained in the surroundings of this minimum so the states do not arrive to be degenerate in this area. It precludes an efficient crossing to lower states, so from this minimum the system can only deactivate by interaction with the environment or by going back to the pedal-like species.

The population of the $\pi\pi^*$ partially rotated local minimum could explain the formation of a bottleneck when azobenzene is excited to S_2, suggested from femtosecond time-resolved spectroscopy[20] on this compound. This suggestion is supported by similar measurements on a rotational constrained derivative,[19] where the bottleneck is not observed. This local minimum can also account for the observed fluorescence from the $\pi\pi^*$ state that correspond to an emission energy of 73.3 kcal·mol^{-1},[22] in good agreement with the 76.7 kcal·mol^{-1} vertical energy difference with the ground state calculated here, although in the referenced work the authors suggest that the species responsible of the emission must be planar.

As a whole, this branch of the relaxation path along the S_2 ($\pi\pi^*$) state explains the low quantum yield of photoisomerization when the initial excitation populates the S_2 state.

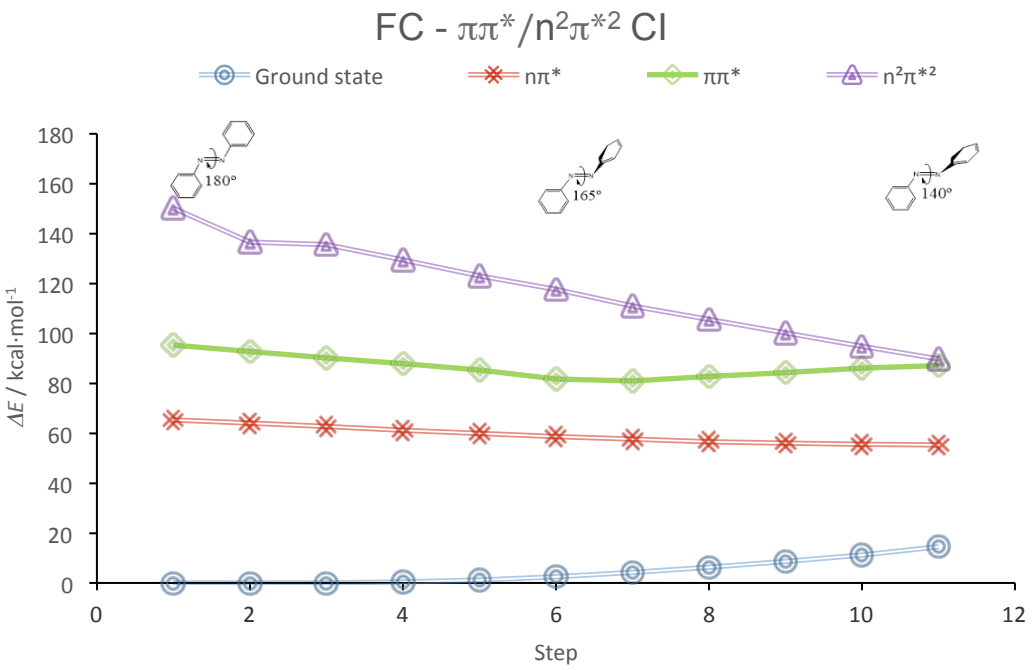

Figure 13. Profiles of the PES of the lowest energy states along the path from the FC geometry to the S_2/S_3 CI.

Mechanism of photoisomerization for systems with constrained rotation

The classical alternative for a non-rotation mechanism is to follow an inversion path, which is the mechanism usually suggested for system with constrained rotation. Along this path, a low energy structure (on S_1 or S_2) with N-N-C angle of 180° could exist. We have searched for such a species on the nπ*, ππ* and $n^2\pi^{*2}$ surfaces, but no stationary point with these characteristics has been located (except the TS on the ground state), so the pure inversion mechanism is ruled out. In fact, this structure has not been reported as an excited state minimum in any of the recent computational papers on this subject.

We also analysed the possibility of a linear C-N-N'-C' structure, related to the concerted-inversion path. This geometry would be favoured by an $n^2\pi^{*2}$ excitation, so we looked for a minimum having the characteristics mentioned. We could not locate such a low-energy critical point, although an energetically-unaffordable linear CI between S_1 and S_0 (energy relative to the ground state minimum: 93 kcal·mol^{-1}) was found as shown in Table 3.

Another alternative for the rotation-constrained mechanism is highlighted by the S_1 (nπ*)/S_0 planar CI located.

The lowest energy geometry of degeneracy found is shown in

Figure 6b. Decay can then occur without rotation but once the system is on the S_0 PES, given the geometry of the crossing point, it does not seem evident that the system will evolve along the S_0 surface to the *cis* isomer. To explore this possibility, the profiles of the lowest excited states along the LIIC from *trans* geometry to S_1/S_0 planar-CI and from here to *cis* geometry were calculated. They are represented in Figure 14. In this LIIC, after the S_1/S_0 CI the phenyl groups rotate step by step to reach the orientation they have at the final *cis* structure, keeping the C-N-N-C moiety in plane.

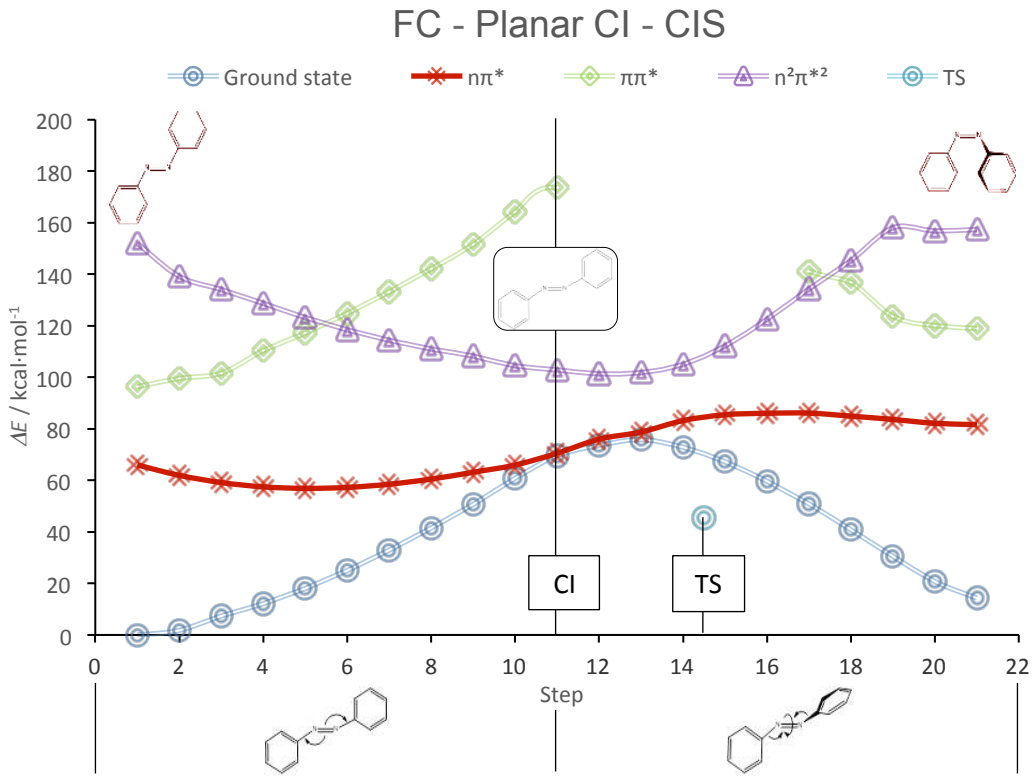

Figure 14. Profiles of the PES of the lowest energy states on a LIIC (non-relaxed path) along planar C-N-N-C geometries for the *trans* → *cis* photoisomerization of azobenzene for system with rotation restricted.

The LIIC shows a small barrier on the S_0 surface (≈6 kcal·mol^{-1}) after the point of decay to S_0, but after studying this feature, we realized that it is in fact an artefact of the route described by the LIIC strategy. To understand it we must recall the thermal isomerization path (along the ground state surface). The transition state we found on S_0 corresponds to the inversion mechanism, with a linear N-N-C moiety and the phenyl rings perpendicular to each other. If the rings are forced to be coplanar, the energy of the structure increases by around 10 kcal·mol^{-1} (Figure 8 and Table 2). In the LIIC of Figure 14, the S_1→S_0 decay geometry (planar CI), has an N-N-C angle of 148°, and the phenyl rings are coplanar. In the next 3 steps of the LIIC the N-N-C angle opens to 180°, and the phenyl rings rotate step by step, but they do not reach a perpendicular orientation until later on along the LIIC. This non-perpendicular orientation of the rings, artificially fixed by the LIIC procedure, increases "unnecessarily" the energy of the S_0 profile. The slightest relaxation of the dihedral angle between phenyl rings will decrease the energy of the system on the S_0 state making the barrier of Figure 14 disappear. In fact, a trial calculation was performed on the point with the highest energy, which showed that a twist of less than 10° on one of the phenyl rings yields a stabilization of more than 15 kcal·mol^{-1}, enough to override the barrier. Unfortunately, it is not possible to reproduce in our calculations the constraints imposed in the experiments for flattened systems, but the results obtained are enough to show that if the planar S_1/S_0 CI is reached, the system can evolve towards the *cis* isomer without further barrier.

The S_1/S_0 planar CI will be the crucial point also on the photoisomerization mechanism when the system is excited to S_2. In this case, depending on the rigidity of the restriction of rotation, the system will have more or less precluded the relaxation following the rotation coordinate towards the local minimum at 160°, but in any case the population of the pedal-like minimum will be favoured. Here the system will decay to S_1 given the small energy gap between these states at this geometry. On the S_1 surface, the relaxation will lead to the S_1 (nπ*)/S_0 planar CI. To check the availability of this path, we calculated the profile of the S_1 (nπ*) surface along the LIIC joining S_2 pedal-like minimum geometry with S_1/S_0 planar CI (Figure 15). The S_1 surface presents a midway pseudo-minimum and, after that, a 14 kcal·mol^{-1} barrier to reach the conical intersection. Given that the energy of excitation to S_2 is more than 25 kcal·mol^{-1} higher than that of this planar CI, this decay path will be easily accessible, and the *cis*-azobenzene photoisomer can be obtained.

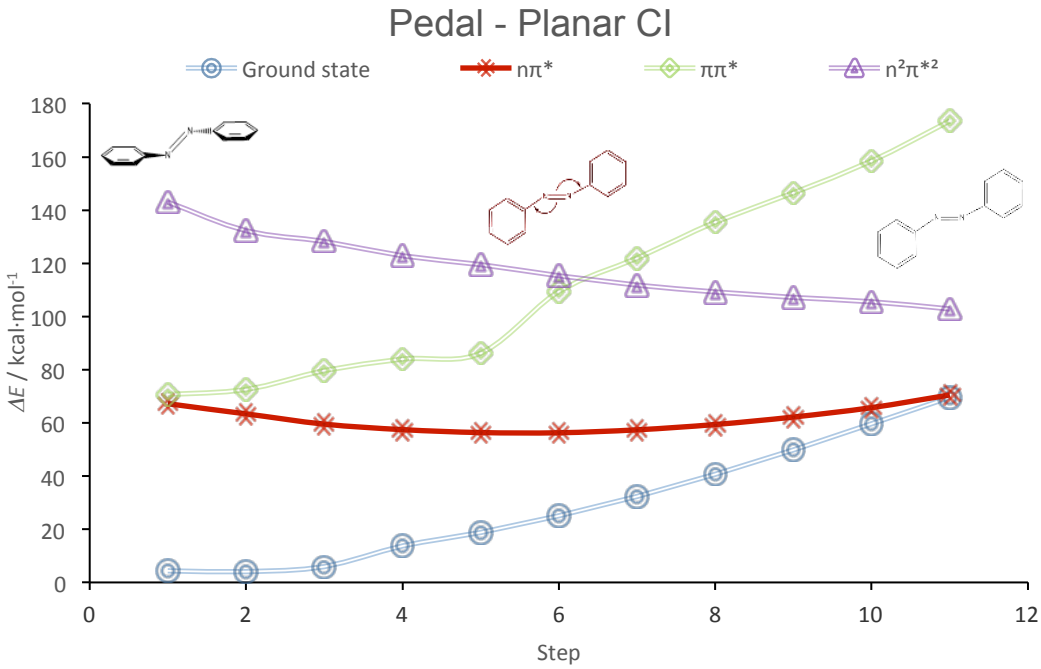

Figure 15. Profiles of the PES of the lowest energy states along the LIIC from the S_2 ($\pi\pi^*$) pedal-like structure to the S_1/S_0 planar CI.

Conclusions

The mechanisms suggested by the analysis of the potential energy surfaces is summarize in the cartoon scheme shown in Figure 16.

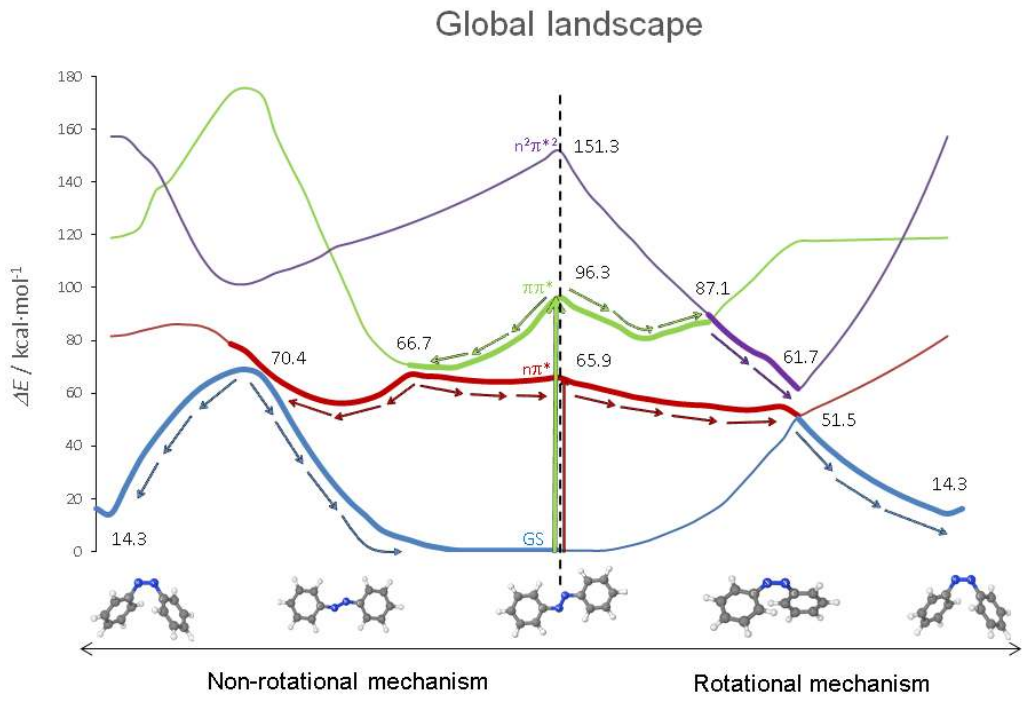

Figure 16. Global scheme of the profiles of the paths for the photoisomerization of azobenzene along S_1 ($n\pi^*$) and S_2 ($\pi\pi^*$) for free-rotation and restricted-rotation azobenzene derivatives (energies, in kcal·mol^{-1}, not in scale).

In systems with free rotation, the minimum energy point of the excited S_1 ($n\pi^*$) has a rotated geometry, which favours the rotational mechanism for photoisomerization along this state. This fact is in agreement with most of the recent computational studies.[34,6-42] Our suggested mechanism includes a crossing point with the ground state located near the S_1 minimum, where the CNNC coordinate reaches the critical value of 90 degrees. On the other hand, for S_2, a new coordinate of relaxation is detected, where the driving force is the out-of-plane concerted distortion of CCNN and NNC'C' dihedral angles in a pedal-like motion. At this distorted geometry S_2 and S_1 are degenerate, so this feature could easily explain the fast deactivation from S_2 to S_1 in planar structures (CNNC=180º), given that this critical point is not far from the ground state geometry of the *trans* isomer, in agreement with the high quantum yields of $S_2 \rightarrow S_1$ internal conversion reported from experimental works.[22,31,38]
From this deactivation point, the most favourable and barrierless pathway goes through the same rotated S_1/S_0 CI used in the S_1 pathway. But the S_2 PES has another downhill coordinate at the FC geometry, less favoured but still possible. It leads to a local minimum with a slightly rotated geometry (CNNC dihedral angle of 165º) and to the nearby crossing with the S_3 state of double-excited $n\pi^*$ character. The possible bifurcation of the relaxation on the S_2 PES could explain the lower quantum yield of photoisomerization when azobenzene is excited to the S_2 ($\pi\pi^*$) state[10,11]
In a constrained environment, when the system is excited to S_2, the relaxation towards the rotated local minimum (at 160º approx.) and the crossing with the S_3 state (at 140º approx.) will be more or less hindered, depending on the rigidity imposed to the system by the constraint. If the rigidity is large, the quantum yield of isomerization through S_2 will increase, given that relaxation on this surface will lead towards the pedal-like minimum and deexcitation to S_1. Such an observation was reported in ref 24. If the constraint allows certain rotation, rotational relaxation will compete with direct deexcitation to S_1 and this quantum yield will hardly change, as reported in references 11 and 25.
Once on the S_1 ($n\pi^*$) state, reached by deactivation from S_2 or from direct excitation to S_1, deactivation to the ground state must take place. Again, depending on the strength of the imposed constraint, the decay will take place at more or less rotated geometries of the conical intersection seam. It means that the internal conversion can occur at any point of a subspace of geometries with different energies depending on the environment of the system, and making difficult the prediction of the quantum yield of this isomerization pathway. In the less favoured case, for planar geometries, the barrier to reach the CI is 14 kcal·mol^{-1}, but the accumulated inertia of the system after the initial excitation should be enough to overcome it. From the planar S_1/S_0 CI, the system can relax towards the *trans* or the *cis* isomers. To evolve towards the second one, phenyl rings must twist to reach the final geometry of the *cis* isomer. This movement makes the barrier on S_0 surface shown in the LIIC of Figure 14 disappear. Nevertheless, given that the *trans* isomer is favoured thermodynamically, the probability of formation of this isomer is larger. These circumstances would explain the low yield of the *trans*→*cis* photoisomerization of azobenzene.
Finally, the thermal back isomerization *cis*→*trans* that takes place along the ground state potential energy surface, will follow a rotational path that shows a barrier of approximately 30 kcal·mol^{-1}. This energy makes this back reaction slow enough to confer long lifetimes to the *cis* isomer.

From the computational point of view, our results show that to determine properly the topology of the potential energy surfaces of the excited states of azobenzene, it is necessary to include in the geometry optimization procedure the dynamic electron correlation, in order to describe accurately enough the electronic distribution of this excited states. This feature of the computational methodology used here has allowed us to locate more accurately than in previous works the critical points crucial to describe the mechanism of photoisomerization of azobenzene.

Acknowledgements

Financial support has been provided by the Spanish Administration (CTQ2014-51938) and the Generalitat de Catalunya (2014SGR199, Xarxa R+D+I en Química Teòrica i Computacional, XRQTC and doctoral grant of J.C.) Additional calculations were run using the Imperial College London High Performance Computing centre.

Keywords: Ab initio calculations • Azo compounds • photoisomerization • reaction mechanisms

[1] G. S. Hartley, *Nature* **1937**, *140*, 281.
[2] Z. Mahimwalla, K. G. Yager, J. Mamiya, A. Shishido, A. Priimagi, C. J. Barrett, Polym. Bull. **2012**, *69*, 967–1006.
[3] J. García-Amorós, D. Velasco, *Beilstein J. Org. Chem.* **2012,** *8,* 1003–1017.
[4] P. P. Birnbaum, J. H. Linford, D. W. G. Style, *Trans. Faraday Soc.* **1953**, *49*, 735.
[5] D. L. Beveridge, H. H. Jaffé, *J. Am. Chem. Soc.* **1966**, *88*, 1948.
[6] V. Cantatore, G. Granucci, M. Persico, *Comp. Theor. Chem.,* **2014**, *126,* 1040–1041.
[7] L. Yu, C. Xu, Y. Lei, C. Zhu, Z. Wen, *Phys. Chem. Chem. Phys.* **2014**, *16*, 25883.
[8] E. M. M. Tan, S. Amirjalayer, S. Smolarek, A. Vdovin, F. Zerbetto, W. J. Buma, *Nat Commun* **2015**, *6*.
[9] I. Conti, M. Garavelli, G. Orlandi, *J. Am. Chem. Soc.* **2008**, *130*, 5216.
[10] J. Griffiths, *Chem. Soc. Rev.* **1972**, *1*, 481.
[11] H. Rau, E. Lueddecke, *J. Am. Chem. Soc.* **1982**,*104*, 1616.
[12] L. B. Jones, G. S. Hammond, *J. Am. Chem. Soc.* **1965**, *87*, 4219.
[13] R. H. Dyck, D. S. McClure, *J. Chem. Phys.* **1962**, *36*, 2326.
[14] E. Fischer, *J. Am. Chem. Soc.* **1968**, *90*, 796.
[15] J. Ronayette, R. Arnaud, P. Lebourgeois, J. Lemaire, *Can. J. Chem.* **1974**, *52*, 1848.
[16] P. Bortolus, S. Monti, *J. Phys. Chem.* **1979**, *83*, 648.
[17] N. Biswas, S.Umapathy, *Chem. Phys. Lett.* **1995**, *236*, 24.
[18] T. Nägele, R. Hoche, W. Zinth, J. Wachtveitl, *Chem. Phys. Lett.* **1997**, *272*, 489.
[19] I. K. Lednev, T. Q. Ye, l. C. Abbott, R. E. Hester, J. N. Moore, *J. Phys. Chem. A,* **1998**, *102*, 9161-9166.
[20] I. K. Lednev, T. Q. Ye, P. Matousek, M. Towrie, P. Foggi, F. V. R. Neuwahl, S. Umapathy, R. E. Hester, J. N. Moore, *Chem. Phys. Lett.* **1998**, *290*, 68.
[21] T. Fujino, T. Tahara, *J. Phys. Chem. A.* **2000**, *104*, 4203.
[22] T. Fujino, S. Y. Arzhantsev, T. Tahara, *J. Phys. Chem. A.* **2001**, *105*, 8123.
[23] S. Monti, G. Orlandi, P. Palmieri, *Chem. Phys.* **1982**, *71*, 87.
[24] P. Bortolus, S.Monti, *J. Phys. Chem.* **1987**, *91*, 5046.
[25] H. Rau, *J. Photochem.* **1984**, *26*, 221.
[26] C. Ciminelli, G. Granucci, M.Persico, *J. Chem. Phys.* **2005**, *123*, 174317.
[27] T. Ishikawa, T. Noro, T. Shoda, *J. Chem. Phys.* **2001**, *115*, 7503.
[28] P. Cattaneo, M. Persico, *Phys. Chem. Chem. Phys.* **1999**, *1*, 4739.
[29] C. W. Chang, Y. C. Lu, T. T. W., E. W. G. Diau, *J. Am. Chem. Soc.* **2004**, *126*, 10109.
[30] H. Satzger, S. Spörlein, C. Root, J. Wachtveitl, W. Zinth, P. Gilch, *Chem.Phys. Lett.* **2003**, *372*, 216.
[31] T. Schultz, J. Quenneville, B. Levine, A. Toniolo, T. J. Martínez, S. Lochbrunner, M. Schmitt, J. P. Shaffer, M. Z. Zgierski, A. J. Stolow, *Am. Chem. Soc.* **2003**, *125*, 8098.
[32] A. Cembran, F. Bernardi, M. Garavelli, L. Gagliardi, G. Orlandi, *J. Am. Chem. Soc.* **2004**, *126*, 3234.
[33] E. W. G. *J.* Diau, *Phys. Chem. A.* **2004**, *108*, 950.
[34] L. Gagliardi, G. Orlandi, F. Bernardi, A. Cembran, M. Garavelli, *Theor. Chem. Acc.* **2004**, *111*, 363.
[35] G. Granucci, M. Persico, *Theor. Chem. Acc.* **2007**, *117*, 1131.
[36] S. Yuan, Y. Dou, W. Wu, Y. Hu, J. Zhao, *J. Phys. Chem. A.* **2008**, *112*, 13326.
[37] Tiberio, G.; Muccioli, L.; Berardi, R.; Zannoni, C. *Chem. Phys. Chem.* **2010**, *11*, 1018.
[38] H. M. D. Bandara, S. C. Burdette, *Chem. Soc. Rev.* **2012**, *41*, 1809.
[39] R. J. Maurer, K. Reuter, *J. Chem. Phys.* **2011**, *135*, 224303.
[40] M. Bockmann, D. Marx, C. Peter, L. D. Site, K. Kremer, N. L. Doltsinis, *Phys. Chem. Chem. Phys.* **2011**, *13*, 7604.
[41] O. Weingart, Z. Lan, A. Koslowski, W. Thiel, *J. Phys. Chem. Lett.* **2011**, *2*, 1506.
[42] J. A. Gámez, O. Weingart, A. Koslowski, W. Thiel, *J. Chem Theory Comput.* **2012**, *8*, 2352−2358.
[43] M. Segado, M. Reguero, *Phys. Chem. Chem. Phys.* **2011**, *13*, 4138–4148.
[44] M. Segado, I. Gómez, M, Reguero, *Phys.Chem.Chem.Phys.* **2016**, *18*, 6861.
[45] J. Finley, P. A. Malmqvist, B. O. Roos and L. Serrano-Andrés, *Chem. Phys. Lett.* **1998**, *288*, 299–306.
[46] N. Forsberg and M.-A. Malqvist, *Chem. Phys. Lett.* **1997**, *274*,196–204.
[47] P. Malmqvist, B. O. Roos, B. Schimmelpfennig, *Chem. Phys. Lett.* **2002**, *357*, 230–240.
[48] F. Aquilante, L. Vico, N. Ferré, G. Ghigo, P. A. Malmqvist, P. Neogrády, T. B. Pedersen, M. Pitonak, M. Reiher and B. O. Roos, et al., *J. Comput. Chem.* **2010**, *31*, 224.
[49] M. J. Bearpak, M. A. Robb, H. B. Schlegel, *Chem. Phys. Lett.* **1994**, *223*, 269-274.
[50] M. J. Frisch, G. W. Trucks, H. B. Schlegel, G. E. Scuseria, M. A. Robb, J. R. Cheeseman, J. A. Montgomery, Jr., T. Vreven, K. N. Kudin, J. C. Burant, J. M. Millam, S. S. Iyengar, J. Tomasi, V. Barone, B. Mennucci, M. Cossi, G. Scalmani, N. Rega, G. A. Petersson et al., Gaussian 03, Revision C.02, Gaussian, Inc., Wallingford, CT, **2004**.
[51] T. Tsuji, H. Takashima, H. Takeuchi, T. Egawa, S. Konaka, *J. Phys. Chem. A* **2001**, *105*, 9347-9353**.**
[52] K. Suwa,J. Otsuki, K. Goto, *J. Phys. Chem. A* **2010,** *114,* 884–890.

Table of Contents

ARTICLE

Rotation vs Inversion?: The mechanism of photoisomerization of azobenzene depends on the initial excitation and on the degree of constraint of the rotation of the system. Multiconfigurational ab initio calculations provide an accurate description of the potential energy surfaces of the excited states of this system when the dynamic electron correlation is included, and allow explaining the experimental observations.

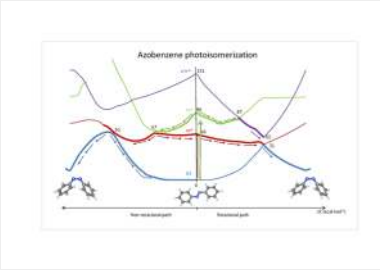

*J. Casellas, M. J. Bearpark, M. Reguero**

Page No. – Page No.

Excited state decay in the photoisomerization of azobenzene: a new balance between mechanisms